Bull. Mater. Sci., Vol. 31, No. 6, November 2008, pp. 885–890. © Indian Academy of Sciences.

Synthesis and characterization of $M_3V_2O_8$ (M = Ca, Sr and Ba) by a solid-state metathesis approach

PURNENDU PARHI, V MANIVANNAN*, SANDEEP KOHLI† and PATRICK McCURDY†

Department of Mechanical Engineering, †Department of Chemistry, Colorado State University, Fort Collins, CO 80523, USA

MS received 24 January 2008; revised 14 February 2008

Abstract. **A solid-state metathesis approach initiated by microwave energy has been successfully applied for the synthesis of orthovanadates, $M_3V_2O_8$ (M = Ca, Sr, and Ba). The structural, vibrational, thermal, optical and chemical properties of synthesized powders are determined by powder X-ray diffraction, scanning electron microscopy, X-ray photoelectron spectroscopy, Fourier transform infrared spectroscopy, differential scanning calorimetry, magnetic property measurements and diffused reflectance spectra in the UV–VIS range. The direct bandgap of the synthesized materials was found to be $3{\cdot}55 \pm 0{\cdot}2$ eV, $3{\cdot}75 \pm 0{\cdot}2$ eV and $3{\cdot}57 \pm 0{\cdot}2$ eV for $Ca_3V_2O_8$, $Sr_3V_2O_8$ and $Ba_3V_2O_8$, respectively.**

Keywords. **Ceramics; chemical synthesis; X-ray microscopy; optical properties; magnetic properties.**

1. Introduction

Many hosts for rare earth ions comprising ternary calcium-oxo-metallates have been studied and $CaWO_4$ is one among them investigated extensively (Brixner and Flournoy 1985). In this regard, the alkaline earth metal orthovanadates, $M_3V_2O_8$ (M = divalent metal), have attracted a lot of attention due to their interesting transport, ferroelectric properties, and use in solid-state lasers (Grzechnik and McMillan 1997a,b; Merkle *et al* 1992; Buijsse *et al* 1995; Zhuravlev and Fotiev 1980). In addition such orthovanadates have found potential usage in television tubes, luminescent lamp coatings and flat panel displays, to name a few.

Among many metal orthovanadates, divalent Ca, Sr and Ba vanadates are of particular interest. For example, calcium orthovanadate, $Ca_3V_2O_8$, belongs to a distorted variant of the $K_2Pb(SO_4)_2$ palmierite structure. It is made up of $[M(XO_4)_2]^{4-}$ layers [M = divalent atom, X = pentavalent atom] linked by M^{2+} cations where the oxygen atoms form a hexagonal close packing. The interlayer site for the Ca^{2+} cation is half occupied with a random distribution of vacancies. The defect structure along with the presence of V^{4+} ions accounts for its high temperature ferroelectric [$T_c \sim 1373$ K] and high electronic conductivity (Glass *et al* 1978; Grzechnik 2002).

Strontium and barium orthovanadates, $Sr_3V_2O_8$ and $Ba_3V_2O_8$, exhibit intense rare earth activated luminescence and when optimized will have intensity of luminescence approaching that of commercially used YVO_4 rare-earth materials (Grzechnik and McMillan 1997a). In addition, near IR-laser action for $Sr_3V_2O_8$ and $Ba_3V_2O_8$ doped with Mn^{5+} at 1168 nm, and 1170 nm have been reported (Merkle *et al* 1992; Buijsse *et al* 1995). Also, barium orthovanadate, due to excellent microwave dielectric properties have been studied for use as microwave filters and antennas (Umemura *et al* 2006).

In general, these important orthovanadates have been synthesized by solid-state reaction using different precursors at high temperatures. The first report of synthesis of $Ca_3V_2O_8$ was carried out by Tammann in 1925 reacting CaO and V_2O_5 (Tammann 1925). Grzechnik and McMillan (1997b) synthesized $Sr_3V_2O_8$ and $Ba_3V_2O_8$ by reacting $SrCO_3$/$BaCO_3$ and V_2O_5 at 1373 K for 72 h. Simner *et al* (2000) synthesized $Sr_3V_2O_8$ by reacting $SrCO_3$ and V_2O_5 at 1423 K for 4 h. Grzechnik and McMillan (1997b) have synthesized $Sr_3V_2O_8$ particles at 1100°C for 72 h. Umemura *et al* (2006) synthesized barium orthovanadate by calcining the precursors at 700°C for 20 h followed by further sintering at high temperature with sintering aid additives. A combustion process followed by post calcination of the products was followed by Zhang *et al* (2006) to produce crystals of Eu doped strontium orthovanadates. These reactions have multi-steps towards product formation and have long reaction times. Therefore, a simplified process that takes less time, and produces crystalline products with high yield is needed.

The solid-state metathesis (SSM) approach is emerging as a viable alternative way of synthesizing inorganic materials of technological importance (Bonneau *et al* 1991). This approach has advantages over the other traditional

*Author for correspondence (mani@engr.colostate.edu)

synthetic methods in terms of reaction rate, with little or no need for external energy. The high lattice energy of the coproduced salt (e.g. NaCl) makes the reaction feasible (Panda *et al* 2003). Previous work by Kaner, Gopalakrishnan, and Parkin has established the versatility of the SSM method to synthesize various inorganic materials including metal pnictides, chalcogenides, carbides, silicides, and borides (Bonneau *et al* 1991; Treece *et al* 1994; Rao *et al* 1995; Gillan and Kaner 1996; Nartowski *et al* 1999; Gopalakrishnan *et al* 2000; Panda *et al* 2003; Mandal and Gopalakrishnan 2005). Metathesis reaction can be initiated by several external sources among which the reactions initiated by microwave radiation are very attractive, since it enables the product formation in a shorter duration of time without generating any residual wastes. Ramanan *et al* have synthesized biologically active hydroxyapatite using the microwave mediated solid-state metathetic route (Parhi *et al* 2004, 2006). We have extended such an approach to synthesize several oxide materials (Parhi *et al* 2008).

The objective of this work is to synthesize orthovanadates of technological importance by a convenient route in contrast to methods commonly found in current literature. Accordingly we have applied the metathesis approach initiated by microwave energy to obtain the desired products. Such an approach to synthesize orthovanadates has not been reported previously. The key advantage with such an approach is that the overall thermal energy associated in the synthesis is less, and the reactions are featured with high yield, easy scalability, and controlled morphology for the final products. We have also determined the optical bandgap of the orthovanadates which has not been reported previously.

2. Experimental

Na_3VO_4, $CaCl_2{\cdot}2H_2O$, $SrCl_2{\cdot}6H_2O$ and $BaCl_2{\cdot}2H_2O$ obtained from Alfa Aesar, USA, were employed for the preparation of the title compounds. Preparation of $Ca_3V_2O_8$ was carried out by reacting $CaCl_2{\cdot}2H_2O$ and Na_3VO_4 in powder form using a domestic microwave oven (2·45 GHz, 1100 W power) for 10 min in the solid-state. The product was washed with water and ethanol and dried at 80°C in an oven. Similar synthetic routes are employed for the synthesis of $Sr_3V_2O_8$ and $Ba_3V_3O_8$ starting from Na_3VO_4 and hydrated MCl_2 (M = Sr, Ba).

Powder X-ray diffraction (XRD) measurements were carried out using Scintag X2 diffractometer with CuK_α radiation. A scan rate of 1 degree/min with a step size of 0·02° was employed to obtain the XRD spectra. Search match analysis was performed using Bruker EVA software. Thermogravimetric analysis (TGA) was performed using the weight and temperature calibrated TA Instruments 2950. The sample was heated in a platinum pan with a heating rate of 10°C/min in order to reach the final temperature. Scanning electron microscopic (SEM) characterization was performed on the JSM-6500F, a field emission system, with the In-Lens Thermal Field Emission Electron Gun. Diffuse reflectance (DR) spectra were recorded in the wavelength range 250–2500 nm using Varian Associates 500 double beam spectrophotometer equipped with a Praying Mantis. Compressed polytetrafluoroethylene was used for standard calibration (100% reflectance). X-ray photoelectron spectroscopy (XPS) experiments were performed on a Physical Electronics 5800 spectrometer. This system has a monochromatic AlK_α X-ray source (h_α = 1486·6 eV), hemispherical analyser, and a multichannel detector. A low energy (30 eV) electron gun was used for charge neutralization on the non-conducting samples. The binding energy (BE) scales for the samples were referenced to the C 1*s* peak at 284·8 eV. Differential scanning calorimetry (DSC) was carried out using TA instruments DSC 2920. The samples were hermetically sealed in aluminum pans and heated to the desired temperature at a ramp rate of 10°C/min.

3. Results and discussion

3.1 *Synthesis of orthovanadates*

Figure 1 shows XRD of the product when $MCl_2{\cdot}xH_2O$ (M = Ca, Sr, Ba) reacted with Na_3VO_4 by solid-state metathesis route as per the reaction,

$$(3CaCl_2{\cdot}2H_2O + 2Na_3VO_4 \xrightarrow{\Delta} Ca_3V_2O_8 + 6NaCl + 2H_2O\uparrow). \quad (1)$$

Figure 1a shows XRD of the product before washing, where Nick (marked with *) coexists with intermediate phases of M–V–O (M = Ca, Sr, Ba) marked with # (JCPDS Card No. 05-0628). The presence of NaCl confirmed the reaction to have proceeded in a metathetic pathway for all the three vanadates, as established in the literature (Bonneau *et al* 1991). The as-synthesized products were washed with water and ethanol to remove the NaCl byproduct and the XRD was taken again. XRD showed an amorphous nature for calcium vanadate, a combination of $Ba_3V_2O_8$ (major phase) and $Ba_4V_2O_9$ for barium vanadate, and a combination of $Sr_3V_2O_8$ (major phase), $Sr_2V_2O_7$ and SrV_2O_4 phases for the corresponding strontium vanadate. In order to find the crystallization temperature for the Ca sample, the sample was subjected to DSC which showed an endothermic peak at 550°C (figure 2). XRD of the sample after DSC as well as a small quantity of the sample subjected to 550°C for 5 h in a furnace showed well-crystalline phase formation of $Ca_3V_2O_8$. Ba and Sr samples were subjected to high temperature heating to find out single-phase formation conditions, which was determined to be 800°C for 3 h. Figures 1b, c and d showed well-crystalline phases of $Ca_3V_2O_8$, $Sr_3V_2O_8$, and $Ba_3V_2O_8$,

respectively in comparison with JCPDS reference patterns (JCPDS Card No. 46-756, 81-1844, 71-2060). Small quantities of impurities were noticed. All the three vanadate phases crystallized in the trigonal system. $Ca_3V_2O_8$ crystallized in the *R*3*c* space group whereas the other two vanadates crystallized in *R-3 m* space group.

In order to understand the influence of various vanadate precursors in the formation of orthovanadates, reactions of hydrated MCl_2 (M = Ca, Sr and Ba) with ammonium vanadate (NH_4VO_3) and sodium vanadate ($NaVO_3$) have been attempted. XRD of the sample showed no reaction between hydrated MCl_2 (M = Ca, Sr and Ba) with either of the precursors. Changing the reaction conditions within the limitations of the domestic microwave (power, reaction time) as well as performing the reaction in solution metathetic pathway (i.e. subjecting the homogeneous solutions of individual precursors in solution) did not yield the desired product formation.

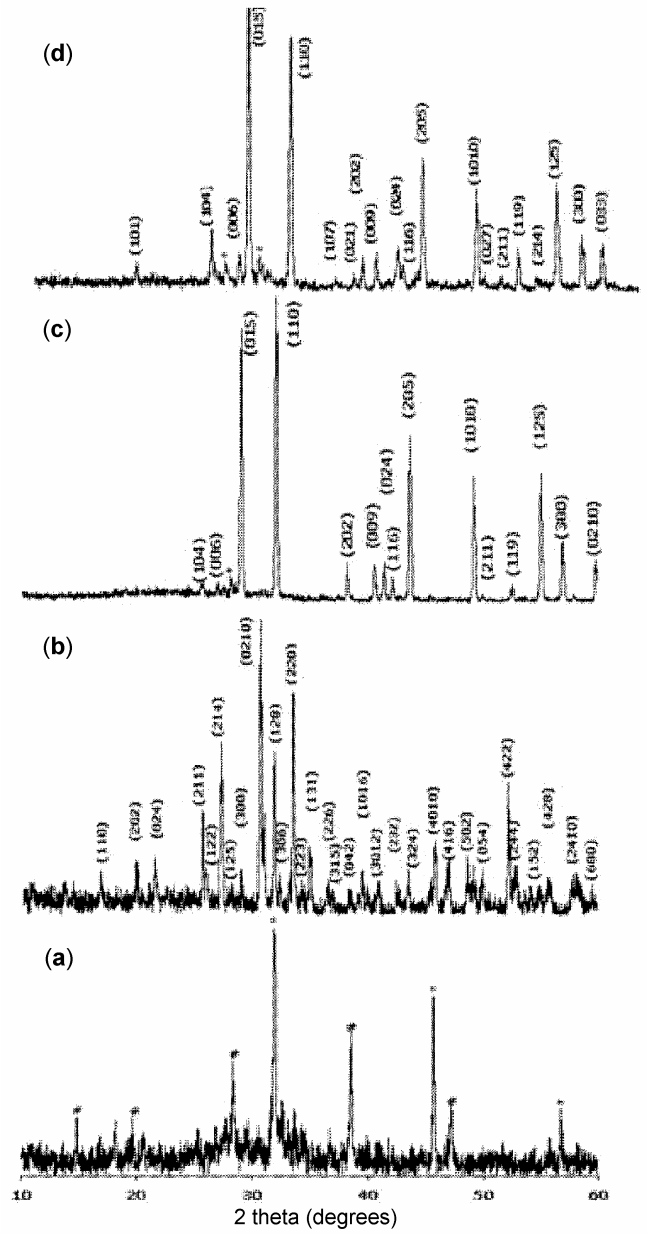

Figure 1. Powder XRD pattern of product before washing, where * corresponds to phases belonging to NaCl confirming the metathesis nature of reactions. Figures 1b, c and d correspond to XRDs of crystalline $Ca_3V_2O_8$,, $Sr_3V_2O_8$ and $Ba_3V_2O_8$, respectively.

3.2 *Characterization of orthovanadates*

Figure 3 shows the SEM morphology of the synthesized $M_3V_2O_8$. SEM showed well defined morphology for all orthovanadates reported in this work. EDX analysis (not shown) confirmed the stoichiometry of the materials. The FTIR spectrum of the $Ca_3V_2O_8$ sample is shown in figure 4. The large isolated absorbable peak around 820 cm^{-1} reveals a typical spectral characteristic of VO_4^{3-} with strong IR absorbable band in the range 780–920 cm^{-1}. The isolated peaks, which contribute to the uniform regular VO_4 tetrahedron, prove the orthovanadate nature of VO_4. Other weak frequencies in the absorbed peaks that appeared in the ranges 3300–3500 and 1600–1650 cm^{-1} are assigned to O–H bonds, which are attributed to surface absorbed water.

XPS (figure 5) was used to probe chemical bonding states of the elements in the range 0–1200 eV. In the spectra of $Ca_3V_2O_8$ (figure 5a), we can see peaks corresponding to V2*s* (628·26 eV), V2*p* (516·26 eV), V3*s* (68·26 eV), V3*p* (41·86 eV), Ca2*s* (437·86 eV), Ca2*p* (346·66 eV) and O1*s* (529·6 eV). In the case of $Sr_3V_2O_8$ (figure 5b), peaks corresponding to different atoms are as follows: V2*s* (629·2 eV), V2*p* (518·8 eV), V3*s* (69·32 eV), V3*p* (42·8 eV), Sr3*s* (58·0 eV), Sr3*d* (135·6 eV), Sr4*s* (64·4 eV), Sr4*p* (20·4) and O1*s* (532·4 eV). In the case of $Ba_3V_2O_8$ (figure 5c), peaks corresponding to different atoms are as follows: Ba3*p* (1062·8 eV), Ba3$d_{3/2}$ (796·4 eV), Ba3$d_{5/2}$ (781·2 eV), Ba4*s* (252·4 eV), Ba4*p* (178·8 eV),

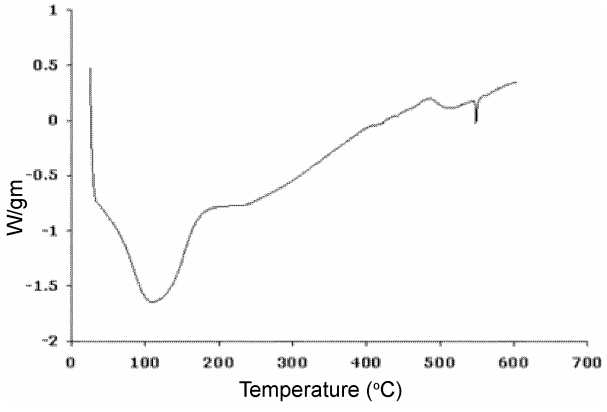

Figure 2. DSC of as-prepared (after washing) $Ca_3V_2O_8$ sample heated up to 600°C.

Ba4*d* (90·4 eV), V2*s* (628·4 eV), V2*p* (517 eV), V3*s* (68·4 eV), V3*p* (41·2 eV) and O1*s* (532·1 eV). XPS data for all the samples confirmed the oxidation state of vanadium to be in + 5 state which is in agreement with the XPS results of single-crystal orthovanadates (Choi *et al* 2006).

3.3 *Physical property measurements*

Orthovanadates have been extensively used as laser-optics materials, where the bandgap (E_g) of the material plays an important role in determining its properties. To determine E_g of the orthovanadates diffuse-reflectance measurements were performed. Figure 6 shows the diffuse reflectance spectra of the $M_3V_2O_8$ sample in the UV–VIS–NIR range. The diffuse reflectance data (figure 6a) was used to calculate the absorption coefficient from the Kubelka–Munk (Kubelka and Munk 1931; Kortum 1969) (KM) function defined as

$$F(R_\infty) = \frac{\alpha}{S} = \frac{(1-R_\infty)^2}{2R_\infty},$$

where

$$R_\infty = \frac{R_{\text{sample}}}{R_{\text{PTFE}}}.$$

Here α is the absorption coefficient, and S the scattering coefficient and $F(R_\infty)$ the KM function. The energy dependence of the material in the UV–VIS–NIR was further explored. The energy dependence of semiconductors near the absorption edge is expressed as

$$\alpha E = K(E - E_g)^\eta.$$

Here E is the incident photon energy ($h\nu$), E_g the optical absorption edge energy, K a constant and exponent η is dependent on the type of optical transition as a result of photon absorption (Barton *et al* 1999). The η is assigned a value of 1/2, 3/2, 2 and 3 for direct allowed, direct forbidden, indirect allowed and indirect forbidden transition, respectively (Tauc *et al* 1966). For the diffuse reflectance spectra, the KM function can be used instead of α for estimation of the optical absorption edge energy (Barton *et al* 1999). It was observed that a plot of $F(R_\infty)E$ vs E was linear near the edge for direct allowed transition (η = 1/2). The intercept of the line on abscissa ($F(R_\infty)E = 0$) gave the value of optical absorption edge energy as 3·55 ± 0·2 eV, 3·75 ± 0·2 eV and 3·57 ± 0·2 eV for $Ca_3V_2O_8$, $Sr_3V_2O_8$ and $Ba_3V_2O_8$, respectively. Figure 6b

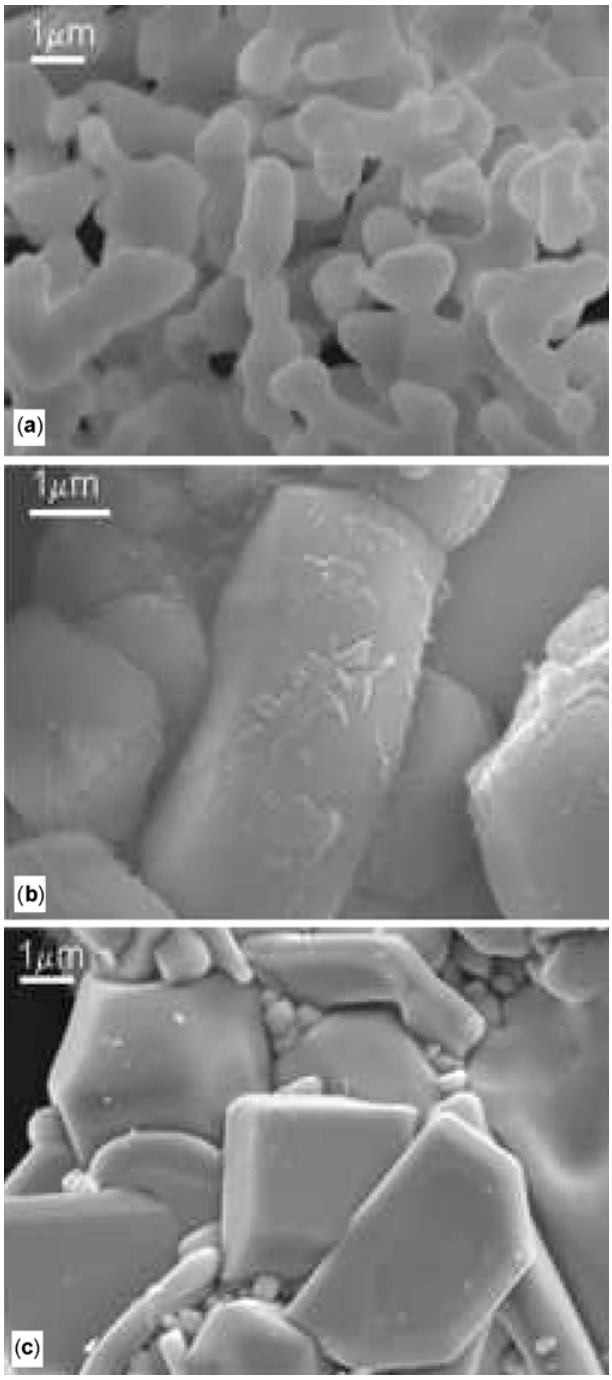

Figure 3. Scanning electron micrograph images of (**a**) $Ca_3V_2O_8$, (**b**) $Sr_3V_2O_8$ and (c) $Ba_3V_2O_8$.

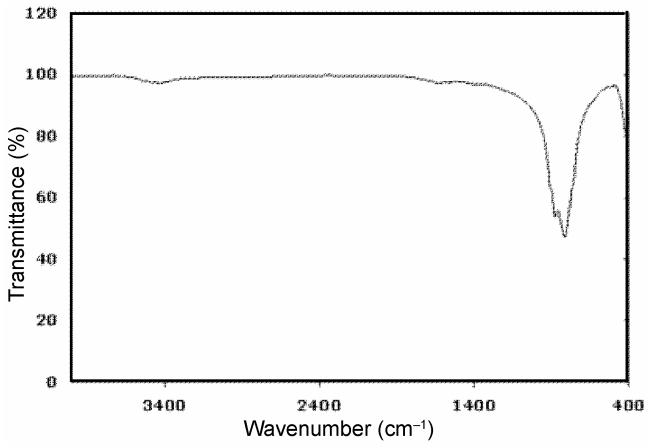

Figure 4. FTIR spectra of $Ca_3V_2O_8$.

shows the plot of the same. The diffuse reflectance spectra for direct bandgap orthorhombic (β) (Sahu and Kleinman 2004) Ta_2O_5 prepared by heating Ta metal in air is also recorded for comparison. The value of optical absorption edge energy for indirect allowed transition for Ta_2O_5 was found to be $4{\cdot}0 \pm 0{\cdot}2$ eV, which is consistent with those seen for the β-Ta_2O_5 reported earlier (Knausenberger and Tauber 1973). The bandgap values determined showed that the orthovanadates synthesized were likely to show semiconducting behaviour.

Magnetic measurements (magnetic susceptibility (χ) as a function of temperature) for orthovanadates (figure 7) showed a diamagnetic response for $Ca_3V_2O_8$ compounds from room temperature to ~ 50 K whereas Ba and Sr analogs showed a paramagnetic response in the same temperature range. The small upturn below 50 K is fitted by a Curie–Weiss expression for $Ca_3V_2O_8$, $Ba_3V_2O_8$ and $Sr_3V_2O_8$, which suggested the presence of a non-orthovanadate phase with $S = 1/2$ for all the three vanadates.

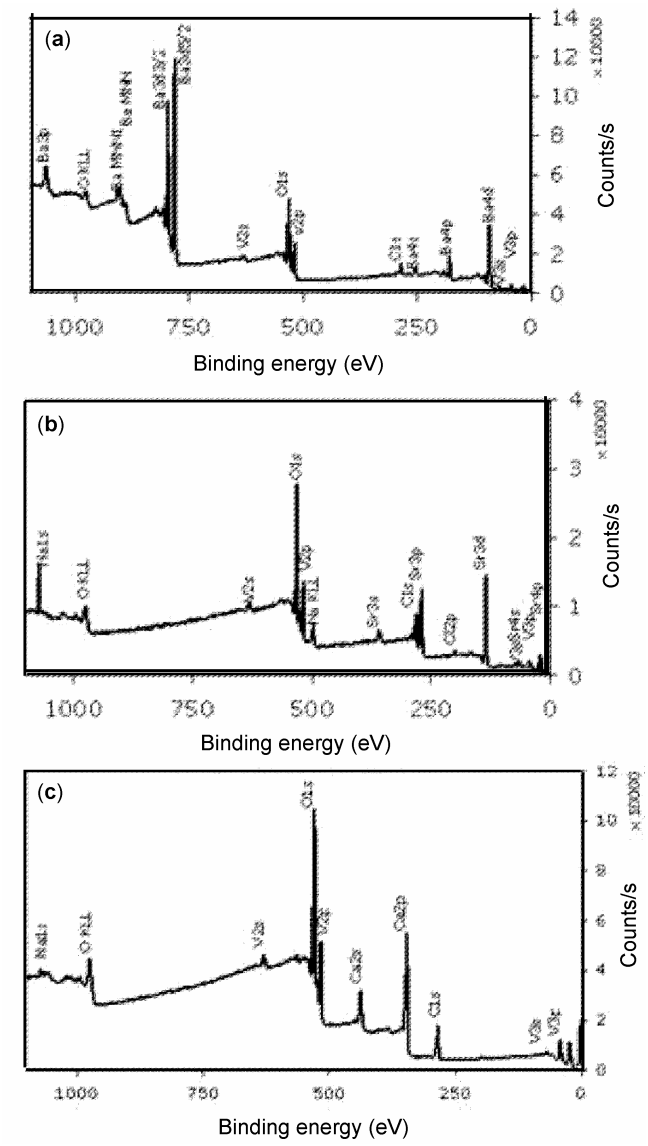

Figure 5. XPS data of (**a**) $Ca_3V_2O_8$, (**b**) $Sr_3V_2O_8$ and (**c**) $Ba_3V_2O_8$.

4. Conclusions

We have successfully synthesized metal vanadates of composition, $M_3V_2O_8$, where M = Ca, Sr, and Ba, by a

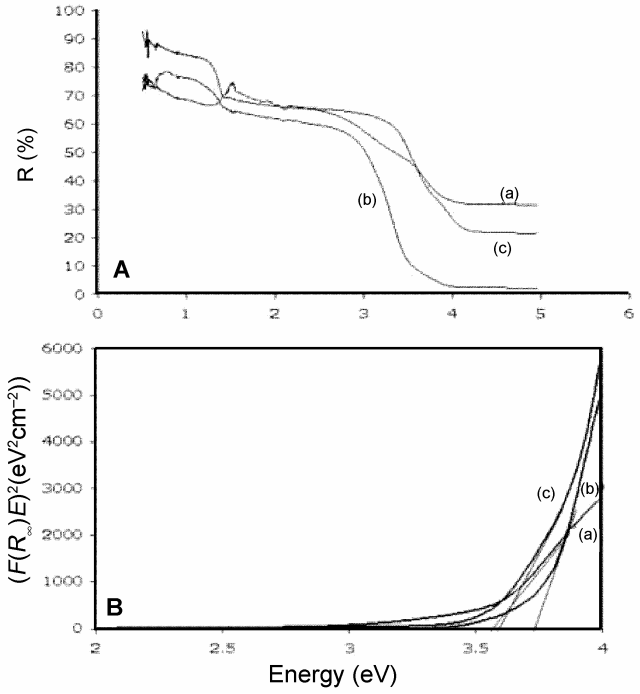

Figure 6. **A**. Diffuse reflectance spectra of (a) $Ca_3V_2O_8$, (b) $Sr_3V_2O_8$ and (c) $Ba_3V_2O_8$, in the wavelength range 250–2500 nm and **B**. plot of $F(R_\infty)$ vs E (eV) for the estimation of the optical absorption edge energy.

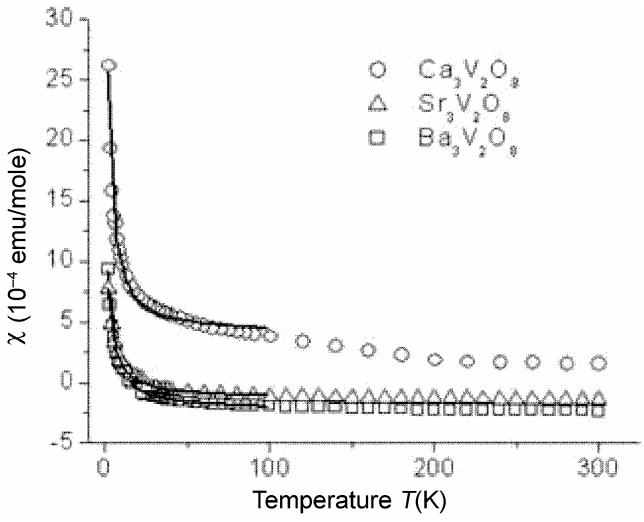

Figure 7. Magnetic susceptibility of $Ca_3V_2O_8$, $Sr_3V_2O_8$ and $Ba_3V_2O_8$ plotted as a function of temperature.

solid state metathesis approach driven by microwave energy and studied the structural, magnetic and optical properties. Such a method of synthesis for orthovanadates has not been reported previously. The proposed method has distinct advantages in terms of cost effectiveness, less complexity, scalability, and high yield. Also, the products have well defined morphologies which will enable them to be used for potential applications including luminescent materials, microwave dielectric materials, and laser optic materials.

Acknowledgements

The authors would like to acknowledge Prof. Allan Kirkpatrick, Department of Mechanical Engineering, CSU, for his continued help, encouragement and support. Thanks are also due to Dr Jaydip Das for help in magnetic measurements.

References

Barton D G, Shtein M, Wilson R D, Soled S L and Iglesia E 1999 *J. Phys. Chem.* **B103** 630

Bonneau P R, Jarvis R F and Kaner R B 1991 *Nature* **349** 510

Brixner L H and Flournoy P A 1985 *J. Elect. Chem. Soc.* **112** 303

Buijsse B, Schmidt J, Chan I Y and Singel D J 1995 *Phys. Rev.* **B51** 6215

Choi J G, Ruy M K, Cho C H, Cho D H, Sung N E, Kim J P and Jang M S 2006 *Ferroelectrics* **332** 29

Gillan E G and Kaner R B 1996 *Chem. Mater.* **8** 333

Glass A M, Abrahams S C, Ballmann A A and Laiacono G 1978 *Ferroelectrics* **17** 579

Gopalakrishnan J, Sivakumar T, Ramesha K, Thangadurai V and Subbanna G N 2000 *J. Am. Chem. Soc.* **122** 6237

Grzechnik A 2002 *Solid State Sci.* **4** 523

Grzechnik A and McMillan P F 1997a *J. Solid State Chem.* **132** 156

Grzechnik A and McMillan P F 1997b *Solid State Commun.* **102** 569

Knausenberger W H and Tauber R N 1973 *J. Electrochem. Soc.* **129** 927

Kortum G 1969 *Reflectance spectroscopy, principles, methods and applications* (New York: Springer-Verlag)

Kubelka P and Munk F 1931 *Z. Tech. Phys.* **12** 593

Mandal T K and Gopalakrishnan J 2005 *Chem. Mater.* **17** 2310

Merkle L D, Pinto A, Verdun H and McIntosh B 1992 *Appl. Phys. Lett.* **61** 2386

Nartowski A M, Parkin I P, MacKenzie M, Craven A J and Macleod I 1999 *J. Mater. Chem.* **9** 1275

Panda M, Seshadri R and Gopalakrishnan J 2003 *Chem. Mater.* **15** 1554

Parhi P, Ramanan A and Ray A R 2004 *Mater. Lett.* **58** 3610

Parhi P, Ramanan A and Ray A R 2006 *Mater. Lett.* **60** 218

Parhi P, Manivannan V, Kohli S and McCurdy P 2008 *Mater. Res. Bull.* (in press)

Rao L, Gillan E G and Kaner R B 1995 *J. Mater. Res.* **10** 353

Sahu B R and Kleinman L 2004 *Phys. Rev.* **B69** 165202

Simner S P, Hardy J S, Stevenson J W and Armstrong T R 2000 *Solid State Ionics* **128** 53

Tammann G 1925 *Z. Anorg. U. Allgem. Chem.* **149** 68

Tauc J, Grigorov R and Vancu A 1966 *Phys. Status Solidi* **15** 627

Treece R E, Conklin J A and Kaner R B 1994 *Inorg. Chem.* **33** 5701

Umemura R, Ogawa H, Yokoi A, Ohsato H and Kan A 2006 *J. Alloy Compd.* **424** 388

Zhang H, Lu M, Yang Z, Xiu Z, Zhou G, Wang S, Zhou Y and Wang S 2006 *J. Alloy Compd.* **426** 384

Zhuravlev V D and Fotiev A A 1980 *Zh. Neorg. Khimii* **25** 2560